HHS Public Access

Author manuscript

J Neuropathol Exp Neurol. Author manuscript; available in PMC 2016 June 01.

Published in final edited form as:

J Neuropathol Exp Neurol. 2015 June ; 74(6): 500–511. doi:10.1097/NEN.0000000000000192.

Spinal Glia Division Contributes to Conditioning Lesion–Induced Axon Regeneration Into the Injured Spinal Cord: Potential Role of Cyclic AMP–Induced Tissue Inhibitor of Metalloproteinase-1

Huaqing Liu, PhD, **Mila Angert, MS**, **Tasuku Nishihara, MD, PhD**, **Igor Shubayev, MD**, **Jennifer Dolkas, BS**, and **Veronica I. Shubayev, MD**

Department of Anesthesiology, University of California, San Diego (HL, MA, TN, JD, VIS); and VA San Diego Healthcare System (HL, MA, TN, IS, JD, VIS), La Jolla, California

Abstract

Regeneration of sensory neurons after spinal cord injury depends on the function of dividing neuronal-glial antigen 2 (NG2)–expressing cells. We have shown that increases in the number of dividing NG2-positive cells through short-term pharmacologic inhibition of matrix metalloproteinases contributes to recovery after spinal cord injury. A conditioning sciatic nerve crush (SNC) preceding spinal cord injury stimulates central sensory axon regeneration via the intraganglionic action of cyclic adenosine monophosphate. Here, using bromodeoxyuridine, mitomycin (mitosis inhibitor), and cholera toxin B tracer, we demonstrate that SNC-induced division of spinal glia is related to the spinal induction of tissue inhibitor of metalloproteinase-1 and contributes to central sensory axon growth into the damaged spinal cord. Dividing cells were mainly NG2-positive and Iba1-positive and included myeloid NG2-positive populations. The cells dividing in response to SNC mainly matured into oligodendrocytes and microglia within the injured spinal cord. Some postmitotic cells remained NG2-reactive and were associated with regenerating fibers. Moreover, intraganglionic tissue inhibitor of metalloproteinase-1 expression was induced after administration of SNC or cyclic adenosine monophosphate analog (dbcAMP) to dorsal root ganglia in vivo and in primary adult dorsal root ganglia cultures. Collectively, these findings support a novel model whereby a cyclic adenosine monophosphate–activated regeneration program induced in sensory neurons by a conditioning peripheral nerve lesion uses tissue inhibitor of metalloproteinase-1 to protect against short-term proteolysis, enabling glial cell division and promoting axon growth into the damaged CNS.

Keywords

Conditioning lesion; Dorsal root ganglia; Microglia; NG2 cell; Oligodendrocyte progenitor; Spinal cord injury; TIMP

Send correspondence and reprint requests to: Veronica I. Shubayev, MD, Department of Anesthesiology, University of California, San Diego, 9500 Gilman Drive, Mail Code 0629, La Jolla, CA 92093-0629; vshubayev@ucsd.edu.

Supplemental digital content is available for this article. Direct URL citations appear in the printed text and are provided in the HTML and PDF versions of this article on the journal's Web site (www.jneuropath.com).

INTRODUCTION

Dorsal root ganglia (DRG) bundle the cell bodies of pseudo-unipolar sensory neurons, projecting their axons into both the peripheral nervous system (PNS) and the central nervous system (CNS). A preceding “conditioning” nerve lesion to the peripheral branch of DRG neurons by sciatic nerve crush (SNC) or axotomy enhances the regenerative capacity of central axons into spinal cord injury (SCI) via the intraganglionic action of cyclic adenosine monophosphate (cAMP) (1–4). A cell-permeable cAMP analog, dbcAMP, partly mimics the effects of peripheral conditioning by launching a robust regenerative transcriptional program in DRG. This intraganglionic regenerative program fosters the intrinsic ability of sensory neurons to extend their central axons into the SCI against the inhibitory action of myelin-associated glycoprotein (MAG) (2, 5).

The matrix metalloproteinase (MMP) family of Zn-dependent endopeptidases (collagenases, gelatinases, matrilysins, stromelysins, and membrane-type MMPs) regulates the cleavage and biologic functions of extracellular and cell membrane proteins (6–8). Short-term therapy using pharmacologic inhibitors of catalytic MMP activity (MMPi; i.e. inhibitors binding zinc in the active site of MMPs) promotes sensorimotor recovery after SCI, at least in part by blocking MMP-9–stimulated vascular instability, immune cell recruitment, neuronal apoptosis, microglial activation, and glial scar formation (9–14). Likewise, catalytic MMP-9 stimulates macrophage-mediated growth cone attack of DRG neurons cultured on inhibitory aggrecan, an in vitro model of sensory axonal dieback (15), and triggers dieback of spinal motor axons in vivo (16). Several MMP family members induced after SCI (17) inhibit DRG axonal growth by proteolytic release of inhibitory MAG residues (18).

Glial progenitor cells expressing neuronal-glial antigen 2 (NG2) proteoglycan are the fifth major cell population in the adult CNS. Unlike other CNS glia (i.e. astrocytes, microglia, and oligodendrocytes), NG2-positive glia form functional glutamatergic and GABAergic synapses with neurons and integrate into neuronal networks (19, 20). In response to SCI, NG2-positive cells rapidly divide to replenish the pool of dying oligodendrocytes and to accomplish remyelination (21–23). In addition, NG2-positive microvascular pericytes, macrophages, and microglia regulate angiogenesis and neuronal survival in CNS lesions (21, 24–27). The roles of NG2-positive cells in generating other glial types (19–21) or in fostering axonal growth (26, 28–30) in the damaged CNS have been a subject of intense debate.

Tissue inhibitors of metalloproteinases (TIMP) inhibit the cleavage activity of MMPs by forming MMP/TIMP dimers with a 1:1 molar stoichiometry (6). Having demonstrated that short-term pharmacologic MMP-9 inhibition stimulates NG2-positive cell division, maturation, remyelination, and functional recovery after SCI (13), we here set out to determine the role of NG2-positive cell division and its correlation with the endogenous expression of tissue inhibitor of metalloproteinase-1 (TIMP-1; a potent MMP-9 inhibitor) in conditioning PNS lesion–induced axon regeneration after SCI. Previously, TIMP-1 has emerged as a factor required for NG2-positive cell viability and maturation in neurosphere cultures and spinal cord myelination (31).

The present study revealed that spinal NG2-positive and Iba1-positive cell division after conditioning PNS injury promoted central axon regeneration into SCI and correlated with elevated TIMP-1 synthesis in the spinal cord and DRG. In addition, dbcAMP stimulation of DRG neurons in vitro and in vivo induced TIMP-1 synthesis. We conclude that TIMP-1 mediates the cAMP-induced regeneration program in sensory neurons and glial function to facilitate central axon growth into the damaged CNS after conditioning PNS injury.

MATERIALS AND METHODS

Reagents and Antibodies

Basic reagents were purchased from Sigma (St Louis, MO), unless indicated otherwise. Bromodeoxyuridine (BrdU; 5-bromo-2′-deoxyuridine) and TIMP-1 from human neutrophil granulocytes were purchased from Calbiochem (San Diego, CA); mitomycin and N^6,2′-*O*-dibutyryladenosine-3′,5′-cyclic monophosphate sodium salt (dbcAMP) were purchased from Sigma; cholera toxin B (CTB) subunit was purchased from List Biological Laboratories (Campbell, CA); and 4′,6-diamidino-2-phenylindole (DAPI) was purchased from Molecular Probes (Eugene, OR). The antibodies used for immunodetection were as follows: monoclonal mouse anti-BrdU (B2531; Sigma) and polyclonal rabbit anti–glial fibrillary acidic protein (GFAP; Z0334; Dako, Carpinteria, CA; for dual labeling with NG2, Iba1, and GFAP); monoclonal rat anti-BrdU (ab6326; Abcam, Cambridge, MA; for dual labeling with O1); polyclonal goat anti-CTB (703; List Biological Laboratories); polyclonal rabbit anti-NG2 (AB5320; EMD Millipore, Billerica, MA); monoclonal mouse anti-O1 (MAB344; Chemicon, Temecula, CA); monoclonal mouse anti-CD11b (MCA618R; Serotec, Raleigh, NC); polyclonal rabbit anti-Iba1 (019-19741; Wako, Richmond, VA); monoclonal mouse rat anti-CD68 (MCA341R; Serotec); polyclonal goat anti–calcitonin gene–related peptide (CGRP; 1720-9007; Biogenesis, Bournemouth, United Kingdom); and polyclonal rabbit anti-S100 (Z0311; Dako).

Animal Procedures

Sprague-Dawley rats (200–225 g, female, n = 56; Harlan Laboratories, Indianapolis, IN) were housed at 22 °C under a 12-hour light/dark cycle with ad libitum access to food and water. Anesthesia was achieved using 4% isoflurane (Baxter, Deerfield, IL) in 55% oxygen or by intraperitoneal injection of a cocktail containing Nembutal (50 mg/mL; Abbott Laboratories, Chicago, IL) and diazepam (5 mg/mL; Steris Laboratories, Mentor, OH) in 0.9% saline (Steris Laboratories). Sciatic nerve crush was performed after bilateral or unilateral exposure of the common sciatic nerve at the midthigh level, followed by nerve crush twice for 20 seconds each using fine forceps. Sham nerve operation included nerve exposure without the lesion. T9 to T10 spinal cord dorsal hemisection (SCDH) was performed on day 7 after bilateral SNC. After T9 to T10 laminectomy, the dura mater was pierced, the spinal cord was exposed, and a pledget of Gelfoam soaked in saline was placed on the exposed cord for 1 minute. Spinal cord dorsal hemisection was performed with a blade stereotaxically positioned to a depth of 1.0 mm, fully severing the dorsal horn and column (13). Sham spinal cord operation included laminectomy without the lesion. Ampicillin (30 mg/kg, i.p.; APP Pharmaceuticals, Schaumberg, IL) was administered daily

for 1 week after SCDH; bladders were expressed twice daily until the animals resumed normal eating and drinking and urinary incontinence ceased.

Bromodeoxyuridine and mitomycin were injected to track and block mitosis, respectively.Bromodeoxyuridine (100 mg/kg) or vehicle (1 mmol/L Tris, 0.8% NaCl, and 0.25 mmol/L ethylenediaminetetraacetic acid [pH 7.4]) was injected intraperitoneally immediately after (day 0) and then on days 2, 4, and/or 6 after SNC. Mitomycin (1 mg/kg) or vehicle (saline) was injected intraperitoneally once on day 2 after SNC. To trace regenerating fibers, we injected intrasciatic CTB (1% in 2 μL volume) bilaterally into the nerve fascicle using a 33-gauge needle (32) 3 days before tissue collection. After unilateral L4 to L5 laminectomy and dorsal root and DRG exposure in naive animals, intra-DRG dbcAMP (50 μg) or vehicle (phosphate-buffered saline [PBS]) was injected into L5 DRG in 2 μL volume using a 33-gauge needle. The overlying muscle was sutured with 4.0 Vicryl, and the skin was closed with surgical staples. Animals were killed using Euthasol (100–150 mg/mL, i.p.; Virbac Animal Health, Fort Worth, TX). All animal procedures were performed according to the PHS Policy on Humane Care and Use of Laboratory Animals, the NIH Guide for the Care and Use of Laboratory Animals, and the protocols approved by the Institutional Animal Care and Use Committee at the VA San Diego Healthcare System.

Cells

Primary DRG cultures were performed using DRG from Sprague-Dawley rats (adult, 10-week-old, female; Harlan Laboratories) and digested with 0.04% collagenase and 0.3% trypsin for 3 hours at 37 °C in Dulbecco modified Eagle medium containing 25 mmol/L Hepes buffer. The single cell suspension was washed with 10% fetal bovine serum containing Dulbecco modified Eagle medium and then with PBS. Cells were plated on poly-D-lysine–coated (100 μg/mL; Sigma) and laminin-coated (5 μg/mL; Sigma) dishes in Neurobasal medium containing 2% B27 (Invitrogen, Life Technologies, Grand Island, NY), glutamine (2 mmol/L; Invitrogen), nerve growth factor (25 ng/mL; Sigma), and 100 U/mL penicillin and 100 μg/mL streptomycin. Cells were fixed and stained for CGRP and neurofilament.

Primary Schwann cells were isolated from the sciatic nerves of Sprague-Dawley rats (postnatal days 1–3; Harlan Laboratories) and purified using 10 μmol/L AraC, antifibronectin Thy1.1 antibody, and rabbit complement (all from Sigma) based on established protocols (33). Schwann cell purity was confirmed using antibodies to S100B. Schwann cells were plated on poly-D-lysine–coated dishes in Dulbecco modified Eagle medium (Gibco) containing 10% fetal bovine serum, 100 U/mL penicillin, 100 μg/mL streptomycin, 21 μg/mL bovine pituitary extract (Clonetics, San Diego, CA), and 4 μmol/L forskolin (Calbiochem) at 37 °C under humidified 5.0% CO_2. Cells were passaged upon confluency and used in 3 to 7 passages. Cells recovered for 3 to 5 days, dbcAMP (500 μmol/L; Sigma) was added to the medium for 24 hours, and lysates were collected by Trizol (Invitrogen) and stored at −80 °C. Samples were analyzed in triplicate in 3 independent experiments.

Quantitative Polymerase Chain Reaction

TaqMan primers and probe containing 5′-FAM reporter for rat TIMP-1 (GenBank NM_053819) and glyceraldehyde 3-phosphate dehydrogenase (GAPDH; GenBank X02231) were obtained from Applied Biosystems (cat. no. Rn01430873_g1) and Biosearch Technologies (Petaluma, CA), respectively, as previously reported (34). Tissues (sciatic nerve, L4/L5 DRG, and spinal cord lumbar enlargement) were stored in RNAlater (Ambion, Life Technologies) at −20 °C until analyzed. Total RNA was harvested using Trizol (Invitrogen) and RNeasy mini kit (Qiagen, Hilden, Germany). Tissues or cells were homogenized in Trizol on ice after chloroform extraction. Each sample was treated with RNase-free DNAse I (Qiagen) to eliminate possible DNA contamination. RNA purity was verified by an OD_{260}/OD_{280} absorption ratio of 1.9 to 2.0. Complementary DNA (cDNA) was synthesized using a Transcriptor First Strand cDNA Synthesis kit (Roche). Gene expression was measured by quantitative real-time polymerase chain reaction (PCR; MX4000; Stratagene, La Jolla, CA) TaqMan assay using 50 ng of cDNA. Amplification conditions included the following: 95 °C for 10 minutes, 95 °C for 30 seconds, and 60 °C for 1 minute for 50 cycles. Samples for target and reference genes were run in duplicate. The control containing no cDNA (“no-template” control) showed the absence of contaminating DNA in analyzed samples. Relative messenger RNA (mRNA) levels were quantified using the $-2_{T}^{\Delta\Delta C}$ method (35). Normalization to GAPDH and fold-change calculation were performed using MxPro software (Agilent Technologies, Santa Clara, CA) (36)

Immunostaining and Morphometry

Animals were perfused with 4% paraformaldehyde, and the spinal cords were isolated, postfixed in 4% paraformaldehyde, rinsed, cryoprotected in graded sucrose, embedded into optimal cutting temperature compound in liquid nitrogen, and cut into 25-μm-thick sections. The sections were rinsed in PBS, hydrolyzed in 2 N HCl in PBS for 30 minutes, digested with 0.01% trypsin for 30 minutes at 37 °C, and washed with PBS. Nonspecific binding was blocked with 10% normal goat serum (1 hour, room temperature) and incubated overnight with primary antibody at 4 °C. After a PBS rinse, Alexa 488 goat anti-mouse or goat anti-rat antibody (green; Invitrogen) was applied (1 hour, room temperature). The second primary antibodies were applied overnight at 4 °C, followed by a PBS rinse and application of Alexa 594 goat anti-rabbit, goat anti-mouse, or donkey anti-goat antibody (red; Invitrogen) (1 hour, room temperature). All primary antibodies were diluted in blocking serum. Signal specificity was controlled by omission or replacement of primary antibody with the respective normal IgG. Nuclei were stained with DAPI (blue). Sections were mounted using SlowFade (Invitrogen). Imaging was performed using a Leica DMR microscope and Openlab 4.04 software (Improvision Inc, Coventry, United Kingdom). Bromodeoxyuridine-positive cells were quantitated in the dorsal horn and dorsal column 1 mm caudal to the T9 to T10 spinal cord (in the intact cord with PNS lesions) or in the SCDH epicenter (±0.5 mm) in mitomycin-treated animals (n = 4–7 animals per group) at every sixth 25-μm-thick transverse section in 3 areas per section at 20× or 40× objective magnification. Cells were considered BrdU-positive when they clearly presented within the nucleus a homogenous or clear punctate labeling pattern. Data are expressed as the number of immunostained cells per

area. Cholera toxin B–labeled axons in the epicenter (±0.5 mm) were counted from a series of 3-in-7 sagittal sections 25 μm thick (32). Data are presented as mean ± SEM.

Statistics

Statistical analyses were performed with KaleidaGraph 4.03 (Synergy Software) or SPSS 16.0 (SPSS) software using 2-tailed unpaired Student *t*-test for comparing 2 groups or using repeated-measures analysis of variance (ANOVA) for comparing 3 or more groups, followed by Tukey-Kramer post hoc test. P values lower than 0.05 were considered significant.

RESULTS

PNS Lesion Stimulates Cell Division in the Spinal Cord

Bilateral SNC has been widely used as conditioning lesion to stimulate regeneration of central sensory axons into the injured spinal cord (37). To determine the effects of bilateral SNC on cell division in the spinal cord, we administered BrdU immediately after (day 0) and then on days 2, 4, and 6 after SNC (Fig. 1A). Bromodeoxyuridine detection and quantitation were performed on day 7 after SNC in the segment 1 mm caudal to the T9 to T10 spinal cord in the dorsal horn and dorsal column, including the gracile nucleus, which receives input from first-order DRG neurons. The overall number of BrdU-positive cells increased 4-fold in the dorsal spinal cord on day 7 after SNC compared with sham operation (Figs. 1B, C).

Conditioning Lesion–Induced Mitosis Promotes Axon Regeneration After SCI

Next, we sought to determine whether spinal cell division stimulated by bilateral SNC influenced central axon regeneration into the injured spinal cord. Bromodeoxyuridine or its vehicle (saline) was injected intraperitoneally immediately after SNC and then 2 days after SNC. Mitomycin (an inhibitor of mitosis) (38) or its vehicle (Ringer's solution) was injected intraperitoneally once on day 2 after SNC (Fig. 2A). Bromodeoxyuridine and mitomycin were administered for only 2 days after SNC to assess the role of cells dividing in response to the conditioning lesion and not SCI itself. Subsequently, T9 to T10 SCDH was performed on day 7 after SNC (4). Regenerating axons were traced using CTB injected bilaterally into the sciatic nerves 3 days before tissue collection. Bromodeoxyuridine and CTB labeling was evaluated in the epicenter of SCDH on day 14 after SCDH, corresponding to day 21 after SNC (Fig. 2A).

The number of BrdU-labeled cells in the injured spinal cord was about 7-fold higher after conditioning lesion (38.4 ± 4.6 cells per area; SNC + Vehicle group; Figs. 2B, C) compared with sham nerve operation (5.7 ± 3.1 cells per area; Sham + Vehicle group; Figs. 2B, C). Mitomycin treatment decreased spinal BrdU incorporation stimulated by conditioning lesion (16.9 ± 4.4 cells per area; SNC + Mitomycin group; Figs. 2B, C). Accordingly, high numbers of regenerating CTB-labeled axons reached into the spinal cord lesion epicenter after conditioning lesion (70.7 ± 17.0 fibers per area; SNC + Vehicle group; Figs. 2B, C), but not the sham-operated group (21.7 ± 3.7 fibers per area; Sham + Vehicle group; Figs. 2B, C). Mitomycin treatment reduced the number of regenerating fibers (16.3 ± 4.3 fibers

per area; SNC + Mitomycin group; Figs. 2B, C) compared with vehicle treatment (70.7 ± 17.0 fibers per area; SNC + Vehicle group; Figs. 2B, C). We conclude that spinal cell mitosis within the first days of a conditioning PNS lesion significantly contributes to central DRG axonal growth.

PNS Lesion Stimulates Division of Spinal NG2-Positive and Iba1-Positive Glia

To identify cell populations in the spinal cord dividing in response to bilateral SNC, we used the phenotypic cell markers NG2 (microvascular pericytes and NG2-positive glia), GFAP (astrocytes), and Iba1 (microglia and macrophages). Bromodeoxyuridine codistribution with the cell markers was quantitated on day 7 after SNC in the segment 1 mm caudal to the T9 to T10 spinal cord in the dorsal horn and dorsal column (Fig. 3A). Cells were considered BrdUpositive when they clearly presented within the nucleus a homogenous or clear punctate labeling pattern, such as that shown in Figure 3B. Of the total BrdU-labeled cell populations in the dorsal spinal cord after bilateral SNC, 70.9% ± 6.9% were NG2-positive cells, 73.5% ± 0.7% were Iba1-positive cells, and only 19.2% ± 5.3% were GFAP-positive cells (Figs. 3C, D). The overlapping populations of BrdU-positive/NG2-positive and BrdU-positive/Iba1-positive cells implied a possibility that NG2-positive/Iba1-positive myeloid cells respond to the PNS lesion.

To identify these myeloid NG2-positive cell populations, we used additional cell markers, including CD11b (also known as macrophage-1 antigen, MAC-1, or integrin αM) expressed on monocytes and microglia and CD68 expressed on macrophages and microglia (Fig. 4). The numbers of NG2-positive/CD11b-positive cells of process-bearing cells with microglial morphology increased after SNC compared with sham nerve operation. In contrast, NG2-positive/CD11b-positive or NG2-positive/CD68-positive cells with morphologic features of macrophages were uncommon in the spinal cord after either SNC or sham nerve operation. Neuronal-glial antigen 2–positive/CD11b-positive or NG2-positive/CD68-positive cells of characteristic round macrophage morphology with ruffled membranes and oblong cell bodies were observed in the spinal cord lesion epicenter on day 3 after T9 to T10 SCDH (Fig. 4) and used as controls (24, 27). Together, these data indicate that, in addition to NG2-positive glia, both NG2-positive and NG2-negative microglia rapidly proliferate in the spinal cord after PNS lesion.

Maturation of Cells Dividing After Conditioning Lesion Within the Injured Spinal Cord

Within the damaged spinal cord, NG2-positive glia mature mainly into oligodendrocytes (23), although there is controversy on their postmitotic fate (19, 20, 39). To determine the maturation fate of cells dividing in response to conditioning SNC within the damaged spinal cord, we injected BrdU intraperitoneally on days 0, 2, 4, and 6 after bilateral SNC (matching Fig. 1), followed by SCDH on day 7 after SNC. Regenerating axons were traced after bilateral CTB injection into the sciatic nerves at 3 days before tissue collection. Bromodeoxyuridine and CTB labeling was evaluated in the SCDH epicenter on day 14 after SCDH, corresponding to day 21 after SNC (Fig. 5A).

In the damaged spinal cord, cells that had divided during a conditioning PNS lesion (mainly NG2-positive and Iba1- positive cells) successfully matured into O1-positive

oligodendrocytes and process-bearing Iba1-positive microglia (Fig. 5B). Consistent with the low numbers of proliferating spinal GFAP-positive cells after SNC, the numbers of postmitotic BrdU-positive/ GFAP-positive populations in the damaged spinal cord were low (Fig. 5B). Some postmitotic cells remained NG2-reactive and associated with regenerating CTB-positive fibers (Fig. 5C). Hence, after a conditioning PNS lesion, NG2-positive glia retained a cycling phenotype for an extended period of time. Interestingly, 3 weeks after conditioning lesion but not sham nerve operation, the levels of activated CD11b-labeled microglia within the damaged spinal cord were exceedingly high, albeit these microglia did not express NG2 (Figure, Supplemental Digital Content 1, http://links.lww.com/NEN/A732).

PNS Lesion Induces Intraganglionic and Spinal TIMP-1 Expression

Our earlier finding of accumulation of dividing NG2-positive cells after short-term pharmacologic MMP-9 inhibition in SCI (13) led us to hypothesize that the increase in spinal NG2-positive cell mitosis after a conditioning PNS lesion related to the expression of the endogenous MMP-9 inhibitor TIMP-1. Thus, we analyzed changes in TIMP-1 mRNA expression after SNC at the injury site, ipsilateral L5 DRG, and ipsilateral dorsal spinal cord (Fig. 6A). Consistent with our earlier findings (40), TIMP-1 mRNA expression at the SNC site increased within day 1 of crush and gradually declined by day 7 after crush (Fig. 6B).

At 7 days after crush (corresponding to the increase in NG2-positive cell mitosis; Fig. 1), TIMP-1 mRNA expression in the spinal cord increased 4.4 times compared with naive spinal cord and increased 3 times compared with the spinal cord obtained at 7 days after sham nerve operation (Fig. 6C). In DRG, TIMP-1 expression increased 3.5 times on day 7 after SNC compared with naive DRG and increased 2.6 times compared with DRG on day 7 after sham nerve operation. This increase in intraganglionic TIMP-1 after PNS injury has been previously reported (40–42). Our data established that increased TIMP-1 synthesis in DRG and spinal cord correlated with increased spinal NG2-positive cell division after PNS lesion.

dbcAMP-Induced TIMP-1 in DRG Neurons In Vivo and In Vitro

In response to PNS lesion, a transient upsurge in intraganglionic cAMP initiates a robust transcriptional program in sensory neurons, promoting the regenerative capacity of their central axons. Intraganglionic injection of the cell-permeable cAMP analog dbcAMP in part mimics this effect of PNS injury (1–3, 5, 43). Thus, we assessed TIMP-1 mRNA expression 48 hours after injection of dbcAMP into the DRG of naive animals (Fig. 7A). Compared with naive DRG, TIMP-1 mRNA increased 11 times after dbcAMP and increased more than 4 times after vehicle (PBS) injection, corresponding to a more than 2-fold increase in TIMP-1 expression in DRG after dbcAMP compared with PBS in vivo ($p < 0.0001$). In contrast, intra-DRG injection of dbcAMP produced a modest (38%; $p = 0.034$) increase in TIMP-1 mRNA in the ipsilateral dorsal spinal cord compared with PBS. Primary adult DRG cultures corroborated the data on DRG in vivo.

Specifically, DRG cultures, which consist mainly of CGRP-positive neurons (Fig. 7B), responded to dbcAMP (500 μmol/L for 24 hours) treatment by a more than 2-fold induction

in TIMP-1 expression compared with control media ($p < 0.05$). In contrast, in primary Schwann cell cultures, dbcAMP induced no significant change in TIMP-1 expression. In aggregate, these data suggest that cAMP induces TIMP-1 expression in sensory neurons as part of a regenerative response to a conditioning PNS lesion.

DISCUSSION

Sensory and motor recovery after SCI can be improved by short-term therapy inhibiting catalytic MMP activity using agents binding Zn ion in the MMP active site (e.g. GM6001 and SB3CT). These pharmacologic MMPi agents act by limiting vascular instability, immune cell recruitment, axonal dieback, neuronal apoptosis, and glial scar formation after SCI (9–16, 44). The efficacy of short-term MMPi administered immediately after SCI is important in limiting the adverse effects of targeting potentially beneficial catalytic MMP functions in wound healing, cell migration, neurite growth, and remyelination (9, 12, 40, 45). Accordingly, short-term and selective inhibition of gelatinases using SB3CT (especially of MMP-9) was sufficient to improve functional recovery after SCI at least in part by stimulating division and subsequent maturation of NG2-positive cells into oligodendrocytes, improving remyelination (13). The present study revealed an increase in spinal expression of a natural MMP-9 inhibitor (TIMP-1) and glial division, including NG2-positive cell division after PNS lesion; the latter contributed to conditioning lesion–induced axonal growth into the damaged spinal cord.

Neuronal-glial antigen 2–positive cells and microglia, but not astrocytes, were the main proliferating cell types in the spinal cord after PNS lesion, in agreement with a previous report (46). Neuronal-glial antigen 2–positive cells represent heterogeneous populations in the CNS, including NG2-positive glia and microvascular pericytes (19). In addition, a number of NG2-positive cells were process-bearing microglia. In contrast, myeloid NG2-positive cells with morphologic features of macrophages were not observed in the intact spinal cord after PNS lesion and were detected only in the SCI epicenter earlier (day 3)—not later (2 weeks)—than injury. Microglial activation was observed within the injured spinal cord 3 weeks after conditioning nerve lesion compared with sham nerve operation, although these microglia did not express NG2. Together, these data suggest that myeloid cells express NG2 only transiently in the CNS (24, 47, 48) perhaps to modulate specific functions, such as division and migration (49). By administering BrdU after nerve crush and before SCI, we targeted the cells dividing in response to the conditioning lesion and not SCI itself. As determined using mitomycin, spinal cell division was critical to central sensory axon regeneration or sprouting into the injured spinal cord. Consistent with the findings of Qiu et al (3), conditioning lesion–induced axonal growth reached the midpoint of the SCI epicenter within 2 weeks of injury. By 6 to 8 weeks after SCI, conditioning lesions trigger axon outgrowth beyond the SCI epicenter (1, 4).

The postmitotic fate of cycling NG2-positive cells in the damaged CNS is still being debated; however, the emerging consensus views these cells mainly as oligodendrocyte progenitors (19, 20, 23). In agreement, numerous postmitotic cells that had divided in response to a conditioning PNS lesion were O1-positive 2 weeks after SCI. Neuronal-glial antigen 2–positive cells have the potential to mature toward a Schwann cell lineage, at least

in vitro (50). A possibility of noncycling mature NG2-positive cells has been considered (21). In our study, a small population of BrdU-positive cells remained NG2-reactive for up to 3 weeks after BrdU injection and associated closely with regenerating axons in the injured spinal cord. Our data suggest that a conditioning PNS lesion creates a reservoir of cycling NG2-positive cells in the spinal cord, which is available later in the course of SCI. This pool of NG2-positive cells may serve to generate oligodendrocytes to support remyelination and, before that, to generate permissive passageways for growing axons (26, 28). Neuronal-glial antigen 2–positive cells are also believed to play a role in synaptic integration and other recovery processes in the damaged CNS (19–21, 51).

Enhanced spinal TIMP-1 gene expression after conditioning lesion correlated with the increased number of dividing NG2-positive cells and microglia in the spinal cord. However, no causal link between TIMP-1 expression and NG2-positive cells or microglia mitosis was established in the present study. Generally, TIMP-1 provides a significant level of neuroprotection by inhibiting MMPs, including MMP-9 (44, 52, 53). Thus, conditioning lesion–induced increase in spinal TIMP-1 preceding SCI would be expected to inhibit short-term antimitogenic MMP-9 function in NG2-positive cells (13) and other detrimental functions immediately after SCI (9–12, 14–16). Important data in support of the essential role of TIMP-1 in NG2-positive cell function were obtained from a small interfering RNA approach in NG2-positive cell cultures and TIMP-1 knockout mice. These studies demonstrated a decline in NG2-positive cell numbers, maturation in neurosphere cultures, and delayed spinal cord myelination associated with TIMP-1 deficiency (31). Tissue inhibitor of metalloproteinase-1 was expressed is astrocytes and microglia but not in NG2-positive cells, at least after SCI (31, 54). In addition to TIMP-1 expression, post-Golgi transport of intraganglionic TIMP-1 to the spinal cord after conditioning lesion presents a valid possibility.

For intraganglionic cAMP to promote sensory axonal growth on inhibitory MAG (2), there should be a mechanism suppressing MMP-induced formation of inhibitory MAG fragments (18). Our finding of cAMP-induced TIMP-1 synthesis in DRG neurons provides a compelling potential mechanism. Accordingly, DRG neurons expressing the regenerative cAMP-dependent activating transcription factor 3 induced TIMP-1 expression after PNS injury (41). The specific signal transduction pathways involved in cAMP regulation of TIMP-1 expression are unknown at present. Although SNC and intraganglionic dbcAMP injection comparably induced TIMP-1 expression in DRG, the effects of nerve crush on the spinal cord were more robust. This is not surprising considering that dbcAMP largely but incompletely mimics the effects of a conditioning PNS lesion (1–3, 43). In Schwann cells, where dbcAMP activates a differentiation program (55), TIMP-1 expression did not depend on dbcAMP (40).

Tissue inhibitor of metalloproteinase-1 displays trophic functions in addition to and independent of MMP inhibition in several cell types, including NG2-positive cells (56, 57). Specifically, recombinant TIMP-1, but not the MMPi GM6001 alone, restored the number of cultured NG2-positive cells lost because of TIMP-1 deficiency (31). The mechanisms for TIMP-1 regulation of NG2-positive cell viability require future investigation. By inhibiting MMP-9 proteolysis, TIMP-1 may promote mitosis or subsequent maturation of myelinating

glia via trophic (e.g. insulin-like growth factor 1, epidermal growth factor, or platelet-derived growth factor) signaling (57, 58). In the context of TIMP-1 excess over MMP-9, TIMP-1 promotes growth cone size but shortens neurite length by inhibiting another MMP (59) or independently of MMPs. The latter action is mediated by direct receptor binding or formation of a cell surface complex with CD44 via a noncatalytic hemopexin domain of proMMP-9 or PEX9 (58). In the context of proMMP-9 excess over TIMP-1, proMMP-9 unencumbered by TIMP-1 may be activated (60), potentially resulting in the release of growth-inhibitory MAG residues (18); this would result in degradation of growth-permissive substrates such as laminin (61) or in promotion of macrophage attack of DRG growth cones (15). Stimulation of DRG neuronal cultures with peptides encoding PEX9 promotes neurite growth also by activation of TrkC/extracellular signal–regulated kinase signaling via low-density lipoprotein receptor–related protein 1 (62). Hemopexin-9 peptide may also foster DRG neurite growth by competitive inhibition of MMP-9 binding to substrates (e.g. MAG and laminin) (63). Overall, the levels of individual MMP and TIMP family members, their isoforms, and their binding partners in spatial and temporal relation to the lesion epicenter, and glial scar are all important factors to consider in designing relevant pharmacologic protocols for SCI therapy.

In conclusion, the present study indicates that division of NG2-positive cells and/or microglia after a conditioning PNS lesion augments the regenerative capacity of central sensory axons during subsequent CNS damage. Intraganglionic TIMP-1 synthesis represents an element of a cAMP-induced regenerative program after PNS lesion (Fig. 8). In turn, TIMP-1 mediates cAMP-stimulated growth by preventing the proteolytic release of inhibitory MAG fragments (2, 18). Post-Golgi transport of neuronal TIMP-1 and TIMP-1 expression in the CNS provide a further permissive milieu for NG2-positive cell viability, mitosis, and/or maturation by MMP inhibition (13) and/or processes that are independent of MMPs (31).

Supplementary Material

Refer to Web version on PubMed Central for supplementary material.

Acknowledgments

This study was supported by the Department of Veterans Affairs Merit Review Award (Grant No. 5IO1BX000638) and the National Institutes of Health Research Project Grant Program (Grant No. 5RO1DE022757 to Veronica I. Shubayev).

REFERENCES

1. Neumann S, Bradke F, Tessier-Lavigne M, Basbaum AI. Regeneration of sensory axons within the injured spinal cord induced by intraganglionic cAMP elevation. Neuron. 2002; 34:885–893. [PubMed: 12086637]
2. Hannila SS, Filbin MT. The role of cyclic AMP signaling in promoting axonal regeneration after spinal cord injury. Exp Neurol. 2008; 209:321–332. [PubMed: 17720160]
3. Qiu J, Cai D, Dai H, et al. Spinal axon regeneration induced by elevation of cyclic AMP. Neuron. 2002; 34:895–903. [PubMed: 12086638]
4. Neumann S, Woolf CJ. Regeneration of dorsal column fibers into and beyond the lesion site following adult spinal cord injury. Neuron. 1999; 23:83–91. [PubMed: 10402195]

5. Cai D, Qiu J, Cao Z, McAtee M, Bregman BS, Filbin MT. Neuronal cyclic AMP controls the developmental loss in ability of axons to regenerate. J Neurosci. 2001; 21:4731–4739. [PubMed: 11425900]
6. Nagase H, Visse R, Murphy G. Structure and function of matrix metalloproteinases and TIMPs. Cardiovasc Res. 2006; 69:562–573. [PubMed: 16405877]
7. Lu P, Takai K, Weaver VM, et al. Extracellular matrix degradation and remodeling in development and disease. Cold Spring Harb Perspect Biol. 2011; 3
8. Page-McCaw A, Ewald AJ, Werb Z. Matrix metalloproteinases and the regulation of tissue remodelling. Nat Rev Mol Cell Biol. 2007; 8:221–233. [PubMed: 17318226]
9. Noble LJ, Donovan F, Igarashi T, Goussev S, Werb Z. Matrix metalloproteinases limit functional recovery after spinal cord injury by modulation of early vascular events. J Neurosci. 2002; 22:7526–7535. [PubMed: 12196576]
10. Hansen CN, Fisher LC, Deibert RJ, et al. Elevated MMP-9 in the lumbar cord early after thoracic spinal cord injury impedes motor relearning in mice. J Neurosci. 2013; 33:13101–13111. [PubMed: 23926264]
11. Yu F, Kamada H, Niizuma K, Endo H, Chan PH. Induction of mmp-9 expression and endothelial injury by oxidative stress after spinal cord injury. J Neurotrauma. 2008; 25:184–195. [PubMed: 18352832]
12. Zhang H, Adwanikar H, Werb Z, Noble-Haeusslein LJ. Matrix metalloproteinases and neurotrauma: Evolving roles in injury and reparative processes. Neuroscientist. 2010; 16:156–170. [PubMed: 20400713]
13. Liu H, Shubayev VI. Matrix metalloproteinase-9 controls proliferation of $NG2^+$ progenitor cells immediately after spinal cord injury. Exp Neurol. 2011; 231:236–246. [PubMed: 21756907]
14. Hsu JY, Bourguignon LY, Adams CM, et al. Matrix metalloproteinase-9 facilitates glial scar formation in the injured spinal cord. J Neurosci. 2008; 28:13467–13477. [PubMed: 19074020]
15. Busch SA, Horn KP, Silver DJ, Silver J. Overcoming macrophage-mediated axonal dieback following CNS injury. J Neurosci. 2009; 29:9967–9976. [PubMed: 19675231]
16. Kaplan A, Spiller KJ, Towne C, et al. Neuronal matrix metalloproteinase-9 is a determinant of selective neurodegeneration. Neuron. 2014; 81:333–348. [PubMed: 24462097]
17. Wells JE, Rice TK, Nuttall RK, et al. An adverse role for matrix metalloproteinase 12 after spinal cord injury in mice. J Neurosci. 2003; 23:10107–10115. [PubMed: 14602826]
18. Milward E, Kim KJ, Szklarczyk A, et al. Cleavage of myelin associated glycoprotein by matrix metalloproteinases. J Neuroimmunol. 2008; 193:140–148. [PubMed: 18063113]
19. Richardson WD, Young KM, Tripathi RB, McKenzie I. NG2-glia as multipotent neural stem cells: Fact or fantasy? Neuron. 2011; 70:661–673. [PubMed: 21609823]
20. Nishiyama A, Komitova M, Suzuki R, Zhu X. Polydendrocytes (NG2 cells): Multifunctional cells with lineage plasticity. Nat Rev Neurosci. 2009; 10:9–22. [PubMed: 19096367]
21. Horner PJ, Thallmair M, Gage FH. Defining the NG2-expressing cell of the adult CNS. J Neurocytol. 2002; 31:469–480. [PubMed: 14501217]
22. McTigue DM, Wei P, Stokes BT. Proliferation of NG2-positive cells and altered oligodendrocyte numbers in the contused rat spinal cord. J Neurosci. 2001; 21:3392–3400. [PubMed: 11331369]
23. Kang SH, Fukaya M, Yang JK, Rothstein JD, Bergles DE. $NG2^+$ CNS glial progenitors remain committed to the oligodendrocyte lineage in postnatal life and following neurodegeneration. Neuron. 2010; 68:668–681. [PubMed: 21092857]
24. Jones LL, Yamaguchi Y, Stallcup WB, Tuszynski MH. NG2 is a major chondroitin sulfate proteoglycan produced after spinal cord injury and is expressed by macrophages and oligodendrocyte progenitors. J Neurosci. 2002; 22:2792–2803. [PubMed: 11923444]
25. Smirkin A, Matsumoto H, Takahashi H, et al. Iba1(+)/NG2(+) macrophage-like cells expressing a variety of neuroprotective factors ameliorate ischemic damage of the brain. J Cereb Blood Flow Metab. 2010; 30:603–615. [PubMed: 19861972]
26. Yang Z, Suzuki R, Daniels SB, Brunquell CB, Sala CJ, Nishiyama A. NG2 glial cells provide a favorable substrate for growing axons. J Neurosci. 2006; 26:3829–3839. [PubMed: 16597737]

27. de Castro R Jr, Tajrishi R, Claros J, Stallcup WB. Differential responses of spinal axons to transection: Influence of the NG2 proteoglycan. Exp Neurol. 2005; 192:299–309. [PubMed: 15755547]
28. Busch SA, Horn KP, Cuascut FX, et al. Adult $NG2^{+}$ cells are permissive to neurite outgrowth and stabilize sensory axons during macrophage-induced axonal dieback after spinal cord injury. J Neurosci. 2010; 30:255–265. [PubMed: 20053907]
29. Ughrin YM, Chen ZJ, Levine JM. Multiple regions of the NG2 proteoglycan inhibit neurite growth and induce growth cone collapse. J Neurosci. 2003; 23:175–186. [PubMed: 12514214]
30. Tan AM, Colletti M, Rorai AT, Skene JH, Levine JM. Antibodies against the NG2 proteoglycan promote the regeneration of sensory axons within the dorsal columns of the spinal cord. J Neurosci. 2006; 26:4729–4739. [PubMed: 16672645]
31. Moore CS, Milner R, Nishiyama A, et al. Astrocytic tissue inhibitor of metalloproteinase-1 (TIMP-1) promotes oligodendrocyte differentiation and enhances CNS myelination. J Neurosci. 2011; 31:6247–6254. [PubMed: 21508247]
32. Lu P, Jones LL, Snyder EY, Tuszynski MH. Neural stem cells constitutively secrete neurotrophic factors and promote extensive host axonal growth after spinal cord injury. Exp Neurol. 2003; 181:115–129. [PubMed: 12781986]
33. Brockes JP, Fields KL, Raff MC. Studies on cultured rat Schwann cells. I. Establishment of purified populations from cultures of peripheral nerve. Brain Res. 1979; 165:105–118. [PubMed: 371755]
34. Shubayev VI, Angert M, Dolkas J, Campana WM, Palenscar K, Myers RR. TNFalpha-induced MMP-9 promotes macrophage recruitment into injured peripheral nerve. Mol Cell Neurosci. 2006; 31:407–415. [PubMed: 16297636]
35. Livak KJ, Schmittgen TD. Analysis of relative gene expression data using real-time quantitative PCR and the 2(−Delta Delta *C*(T)) method. Methods. 2001; 25:402–408. [PubMed: 11846609]
36. Pfaffl MW. A new mathematical model for relative quantification in real-time RT-PCR. Nucleic Acids Res. 2001; 29:e45. [PubMed: 11328886]
37. Kadoya K, Tsukada S, Lu P, et al. Combined intrinsic and extrinsic neuronal mechanisms facilitate bridging axonal regeneration one year after spinal cord injury. Neuron. 2009; 64:165–172. [PubMed: 19874785]
38. Liu H, Kim Y, Chattopadhyay S, Shubayev I, Dolkas J, Shubayev VI. Matrix metalloproteinase inhibition enhances the rate of nerve regeneration in vivo by promoting dedifferentiation and mitosis of supporting Schwann cells. J Neuropathol Exp Neurol. 2010; 69:386–395. [PubMed: 20448483]
39. Dawson MR, Polito A, Levine JM, Reynolds R. NG2-expressing glial progenitor cells: An abundant and widespread population of cycling cells in the adult rat CNS. Mol Cell Neurosci. 2003; 24:476–488. [PubMed: 14572468]
40. Kim Y, Remacle AG, Chernov AV, et al. The MMP-9/TIMP-1 axis controls the status of differentiation and function of myelin-forming Schwann cells in nerve regeneration. PLoS One. 2012; 7:e33664. [PubMed: 22438979]
41. Huang B, Zhao X, Zheng LB, Zhang L, Ni B, Wang YW. Different expression of tissue inhibitor of metalloproteinase family members in rat dorsal root ganglia and their changes after peripheral nerve injury. Neuroscience. 2011; 193:421–428. [PubMed: 21782897]
42. Rodriguez Parkitna J, Korostynski M, Kaminska-Chowaniec D, et al. Comparison of gene expression profiles in neuropathic and inflammatory pain. J Physiol Pharmacol. 2006; 57:401–414. [PubMed: 17033093]
43. Blesch A, Lu P, Tsukada S, et al. Conditioning lesions before or after spinal cord injury recruit broad genetic mechanisms that sustain axonal regeneration: Superiority to cAMP-mediated effects. Exp Neurol. 2012; 235:162–173. [PubMed: 22227059]
44. Rosenberg GA. Matrix metalloproteinases and their multiple roles in neurodegenerative diseases. Lancet Neurol. 2009; 8:205–216. [PubMed: 19161911]
45. Krekoski CA, Neubauer D, Graham JB, Muir D. Metalloproteinase-dependent predegeneration in vitro enhances axonal regeneration within acellular peripheral nerve grafts. J Neurosci. 2002; 22:10408–10415. [PubMed: 12451140]

46. Echeverry S, Shi XQ, Zhang J. Characterization of cell proliferation in rat spinal cord following peripheral nerve injury and the relationship with neuropathic pain. Pain. 2008; 135:37–47. [PubMed: 17560721]
47. Bu J, Akhtar N, Nishiyama A. Transient expression of the NG2 proteoglycan by a subpopulation of activated macrophages in an excitotoxic hippocampal lesion. Glia. 2001; 34:296–310. [PubMed: 11360302]
48. Sugimoto K, Nishioka R, Ikeda A, et al. Activated microglia in a rat stroke model express NG2 proteoglycan in peri-infarct tissue through the involvement of TGF-β1. Glia. 2014; 62:185–198. [PubMed: 24311432]
49. Makagiansar IT, Williams S, Mustelin T, Stallcup WB. Differential phosphorylation of NG2 proteoglycan by ERK and PKCalpha helps balance cell proliferation and migration. J Cell Biol. 2007; 178:155–165. [PubMed: 17591920]
50. Zawadzka M, Rivers LE, Fancy SP, et al. CNS-resident glial progenitor/stem cells produce Schwann cells as well as oligodendrocytes during repair of CNS demyelination. Cell Stem Cell. 2010; 6:578–590. [PubMed: 20569695]
51. Polito A, Reynolds R. NG2-expressing cells as oligodendrocyte progenitors in the normal and demyelinated adult central nervous system. J Anat. 2005; 207:707–716. [PubMed: 16367798]
52. Tejima E, Guo S, Murata Y, et al. Neuroprotective effects of overexpressing tissue inhibitor of metalloproteinase TIMP-1. J Neurotrauma. 2009; 26:1935–1941. [PubMed: 19469687]
53. Tan HK, Heywood D, Ralph GS, Bienemann A, Baker AH, Uney JB. Tissue inhibitor of metalloproteinase 1 inhibits excitotoxic cell death in neurons. Mol Cell Neurosci. 2003; 22:98–106. [PubMed: 12595242]
54. Welser-Alves JV, Crocker SJ, Milner R. A dual role for microglia in promoting tissue inhibitor of metalloproteinase (TIMP) expression in glial cells in response to neuroinflammatory stimuli. J Neuroinflamm. 2011; 8:61.
55. Jessen KR, Mirsky R. Schwann cells and their precursors emerge as major regulators of nerve development. Trends Neurosci. 1999; 22:402–410. [PubMed: 10441301]
56. Stetler-Stevenson WG. Tissue inhibitors of metalloproteinases in cell signaling: Metalloproteinase-independent biological activities. Sci Signal. 2008; 1:re6. [PubMed: 18612141]
57. Moore CS, Crocker SJ. An alternate perspective on the roles of TIMPs and MMPs in pathology. Am J Pathol. 2012; 180:12–16. [PubMed: 22033229]
58. Lambert E, Bridoux L, Devy J, et al. TIMP-1 binding to proMMP-9/CD44 complex localized at the cell surface promotes erythroid cell survival. Int J Biochem Cell Biol. 2009; 41:1102–1115. [PubMed: 19010442]
59. Ould-yahoui A, Tremblay E, Sbai O, et al. A new role for TIMP-1 in modulating neurite outgrowth and morphology of cortical neurons. PLoS One. 2009; 4:e8289. [PubMed: 20011518]
60. Goldberg GI, Strongin A, Collier IE, Genrich LT, Marmer BL. Interaction of 92-kDa type IV collagenase with the tissue inhibitor of metalloproteinases prevents dimerization, complex formation with interstitial collagenase, and activation of the proenzyme with stromelysin. J Biol Chem. 1992; 267:4583–4591. [PubMed: 1311314]
61. Gu Z, Cui J, Brown S, et al. A highly specific inhibitor of matrix metalloproteinase-9 rescues laminin from proteolysis and neurons from apoptosis in transient focal cerebral ischemia. J Neurosci. 2005; 25:6401–6408. [PubMed: 16000631]
62. Yoon C, Van Niekerk EA, Henry K, et al. Low-density lipoprotein Receptor–related protein 1 (LRP1)–dependent cell signaling promotes axonal regeneration. J Biol Chem. 2013; 288:26557–26568. [PubMed: 23867460]
63. Roeb E, Schleinkofer K, Kernebeck T, et al. The matrix metalloproteinase 9 (mmp-9) hemopexin domain is a novel gelatin binding domain and acts as an antagonist. J Biol Chem. 2002; 277:50326–50332. [PubMed: 12384502]

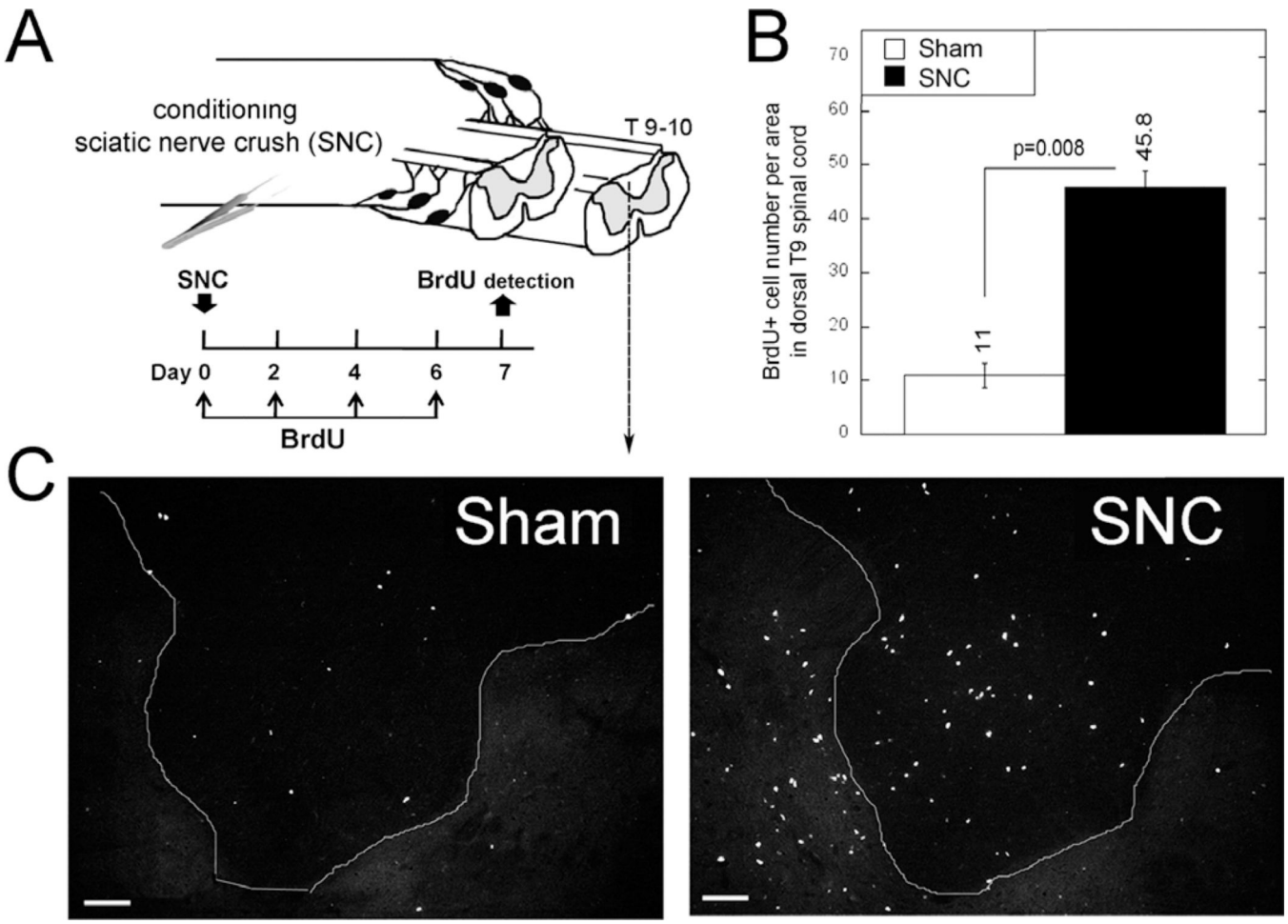

FIGURE 1.

Spinal cell proliferation after PNS injury. **(A)** Experimental schedule and schematic diagram. Bromodeoxyuridine (50 mg/kg/day, i.p.) or vehicle was injected on days 0, 2, 4, and 6 after unilateral SNC and detected in the ipsilateral dorsal T9 to T10 spinal cord on day 7 after SNC or sham nerve operation. **(B)** Mean ± SEM BrdU-positive cell numbers in transverse sections, following **(A)** (n = 4 animals per group, 5–7 sections per n, spaced 125 μm apart, per 55–103 μm^2; p value by Student t-test). **(C)** Bromodeoxyuridine-positive micrographs representative of data in **(B)**. Scale bar = 50 μm.

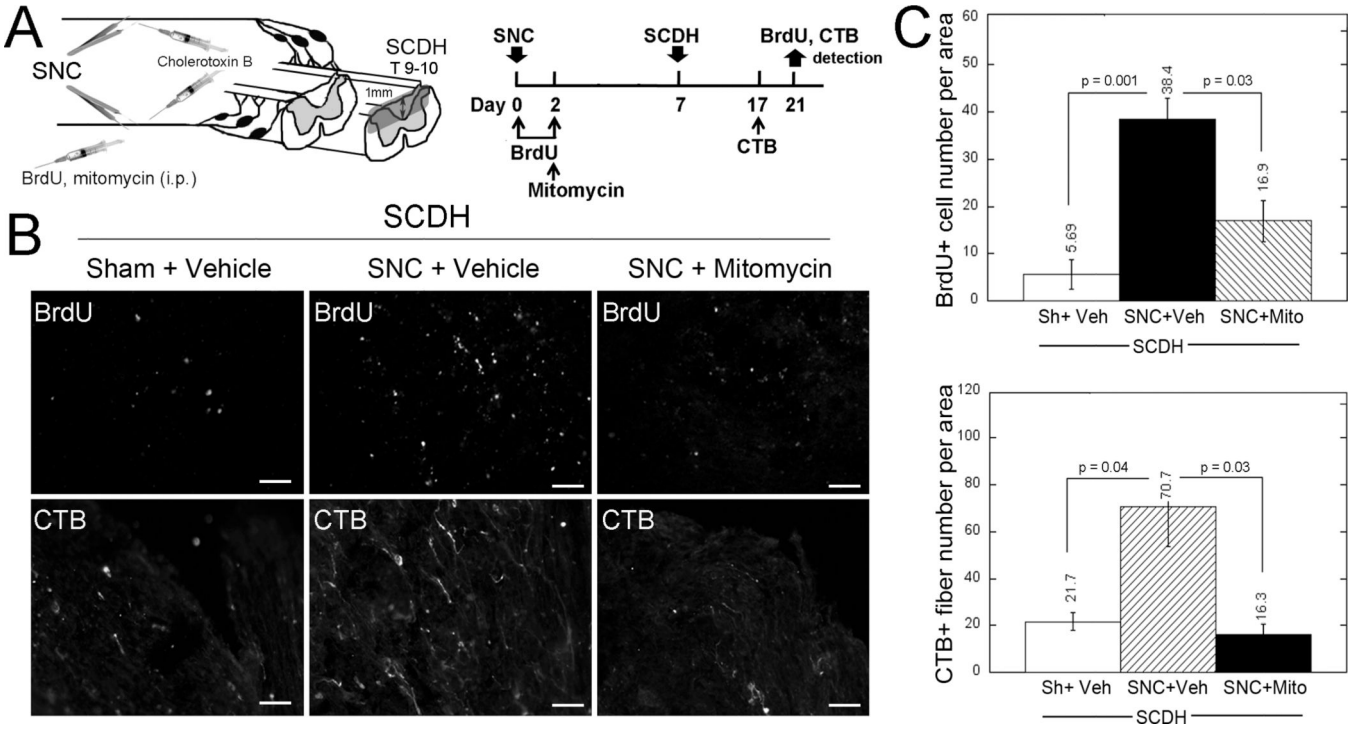

FIGURE 2.

Blockade of spinal cell proliferation with mitomycin (Mito) inhibits conditioning lesion–induced central axon growth into injured spinal cord. **(A)** Experimental schedule and schematic diagram: BrdU (50 mg/kg/day, i.p.) or vehicle (Veh) was injected on days 0 and 2 after bilateral SNC, followed by Mito (1 mg/kg, i.p.) injection on day 2 after SNC. T9 to T10 SCDH was performed on day 7 after SNC. Regenerating fibers were traced using bilateral intrasciatic injection of CTB (1% in 2 μL volume) on day 17 after SNC. Bromodeoxyuridine and CTB were detected on day 21 after SNC, corresponding to day 14 after SCDH. **(B)** Bromodeoxyuridine (B2531) and CTB immunostaining in the SCDH epicenter, following **(A)**. Representative micrographs of 5 animals per group. Scale bar = 50 μm. **(C)** Mean ± SEM BrdU-positive cell numbers or CTB-positive fibers per 55- to 103-μm^2 area in longitudinal spinal cord sections, following **(A, B)** (n = 5 animals per group, 5–7 sections per n, spaced 125 μm apart; p values by 1-way ANOVA and Tukey post hoc test). Sh, Sham.

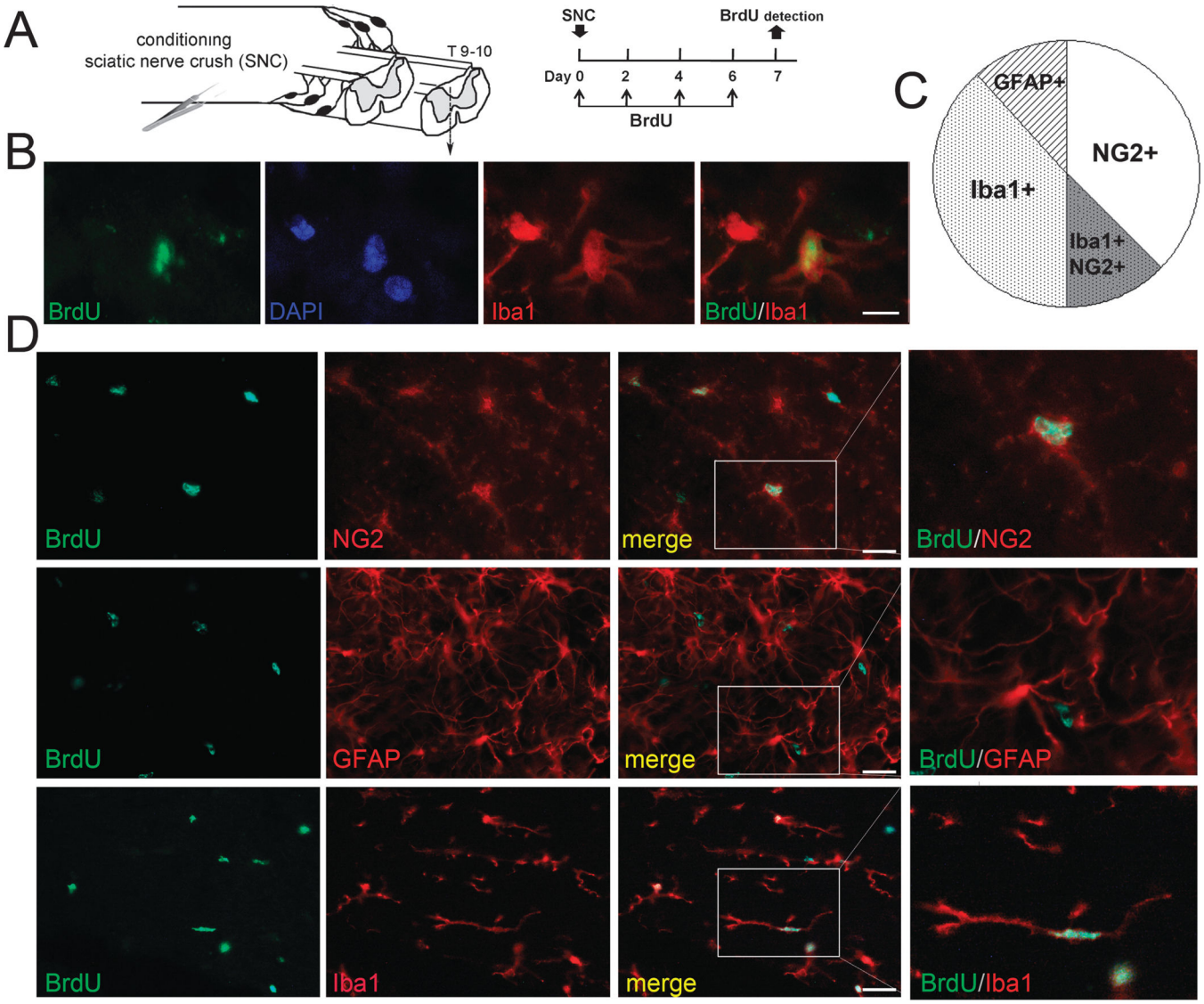

FIGURE 3.

Spinal NG2-positive and Iba1-positive cells proliferate after PNS injury. **(A)** Experimental schedule and schematic diagram. Bromodeoxyuridine (50 mg/kg/day, i.p.) or vehicle was injected on days 0, 2, 4, and 6 after unilateral SNC and detected in the ipsilateral dorsal T9 to T10 spinal cord on day 7 after SNC or sham nerve operation. **(B)** Dual staining for BrdU (green; B2531) and Iba1 (red), following **(A)**. DAPI, blue. Scale bar = 10 μm. **(C)** Pie chart representing the mean BrdU-positive cell numbers dual-labeled with anti-NG2, anti-Iba1, or anti-GFAP antibodies, expressed as percentage of total BrdU-positive cells. **(D)** Dual staining for BrdU (green; B2531) and NG2, Iba1, or GFAP (red), following **(A)**, and representative micrographs of **(D)**. Scale bar = 25 μm.

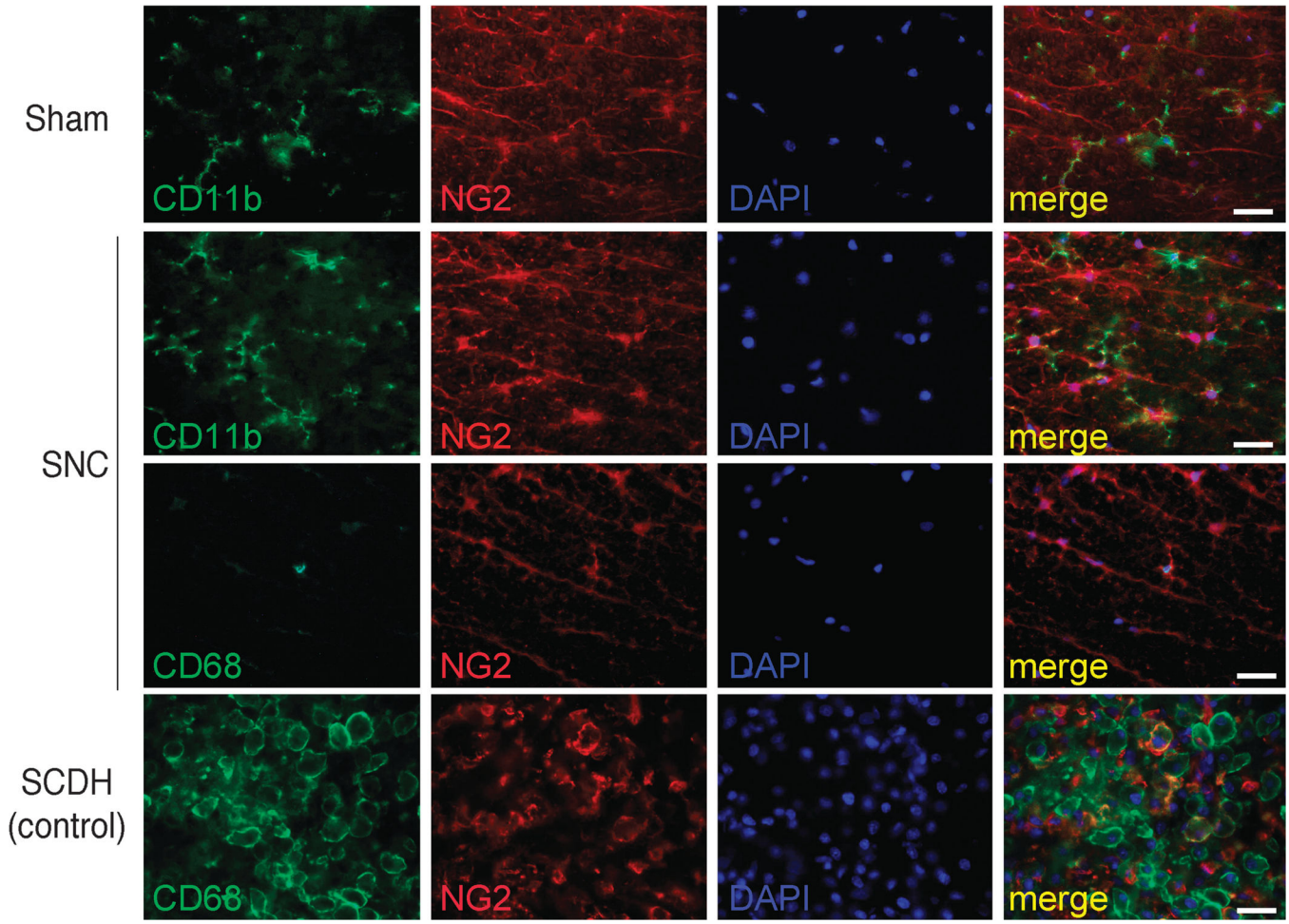

FIGURE 4.

Myeloid NG2-positive cells in the spinal cord. Dual staining for NG2 (red) with anti-CD11b or anti-CD68 (green) antibodies in the dorsal spinal cord on day 7 after bilateral SNC or sham nerve operation. T9 to T10 SCDH (epicenter; day 3) is used as positive control. Process-bearing NG2-positive/CD11b-positive cell (presumably microglia) numbers increased after SNC compared with sham. Neuronal-glial antigen 2–positive/CD68-positive cells (macrophages/microglia) are few in the SNC and Sham groups (SNC is shown). In contrast to the spinal cord associated with SNC, the direct SCDH lesion epicenter displays numerous NG2/CD68-positive cells with morphologic features of macrophages. DAPI, blue. Representative micrographs of 3 animals per group. Scale bar = 25 μm.

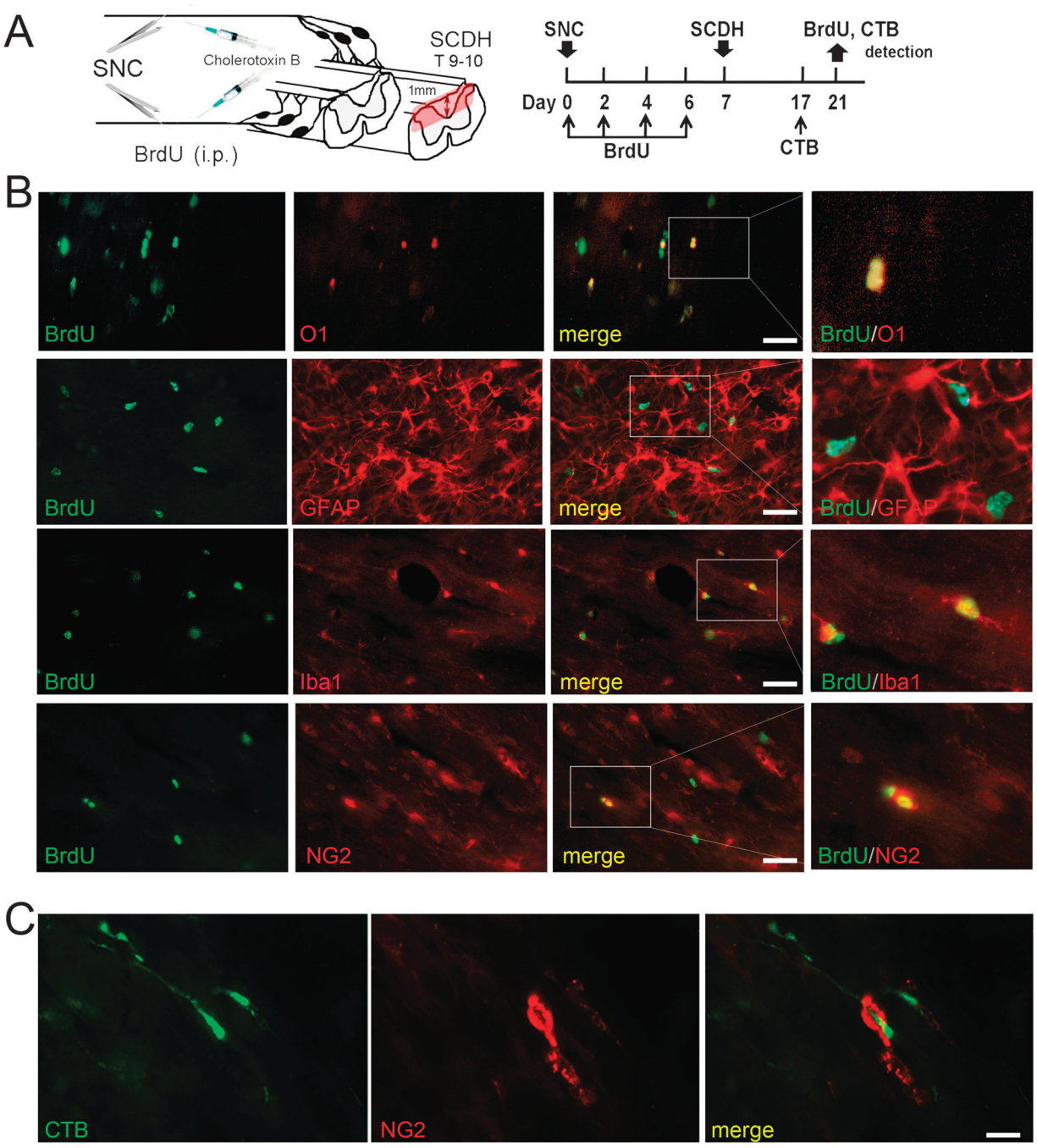

FIGURE 5.

Maturation of conditioning lesion–stimulated cells in SCI. **(A)** Experimental schedule and schematic diagram. Bromodeoxyuridine (50 mg/kg/day, i.p.) or vehicle was injected on days 0, 2, 4, and 6 after bilateral SNC. T9 to T10 SCDH was performed on day 7 after SNC. Regenerating fibers were traced using bilateral intrasciatic injection of CTB subunit (1%) on day 17 after SNC. Bromodeoxyuridine and CTB were detected on day 21 after SNC, corresponding to day 14 after SCDH. **(B)** Dual labeling for BrdU (green; ab6326) with O1 (red) and for BrdU (green; B2531) with anti-Iba1, anti-NG2, or anti-GFAP (red) antibodies

in longitudinal sections at the SCDH epicenter, following **(A)**. **(C)** Dual staining for CTB (green) and NG2 (red) in the spinal cord, following **(A)**. Representative micrographs of 5 animals per group. Scale bars = **(B)** 35 μm; **(C)** 15 μm.

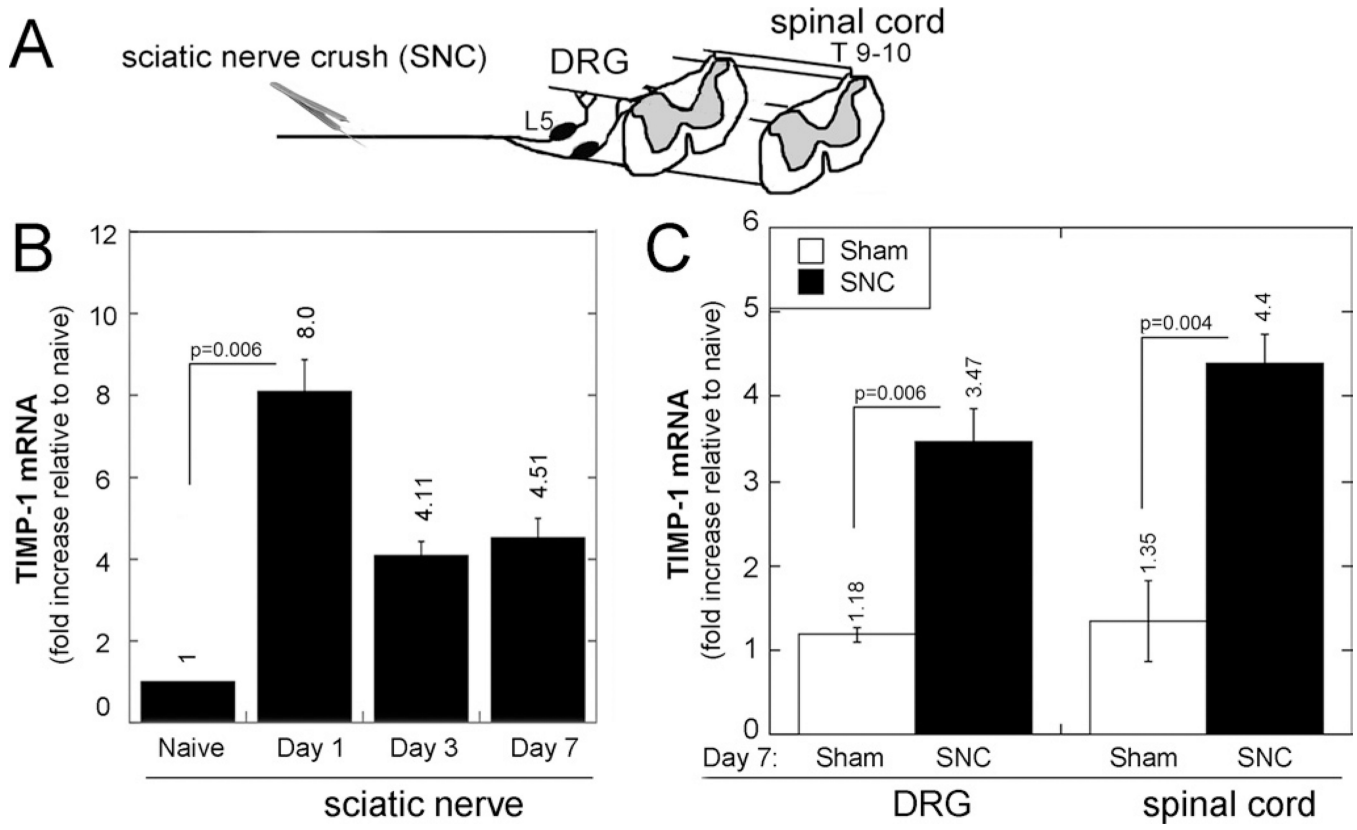

FIGURE 6.

Intraganglionic and spinal TIMP-1 after SNC. **(A–C)** TaqMan quantitative PCR for TIMP-1 after SNC or sham nerve operation, analyzed in sciatic nerve, ipsilateral L4/L5 (pooled) DRG, and lumbar spinal cord, as shown in experimental schema **(A)**. Tissue inhibitor of metalloproteinase-1 expression was first analyzed on days 1, 3, and 7 after SNC in sciatic nerve **(B)** and then in DRG and spinal cord on day 7 after SNC or sham operation **(C)**. Graphs represent the mean ± SEM relative mRNA expression of 4 to 6 animals per group, normalized to GAPDH and calibrated to naive tissues (p values by 1-way ANOVA and Tukey post hoc test).

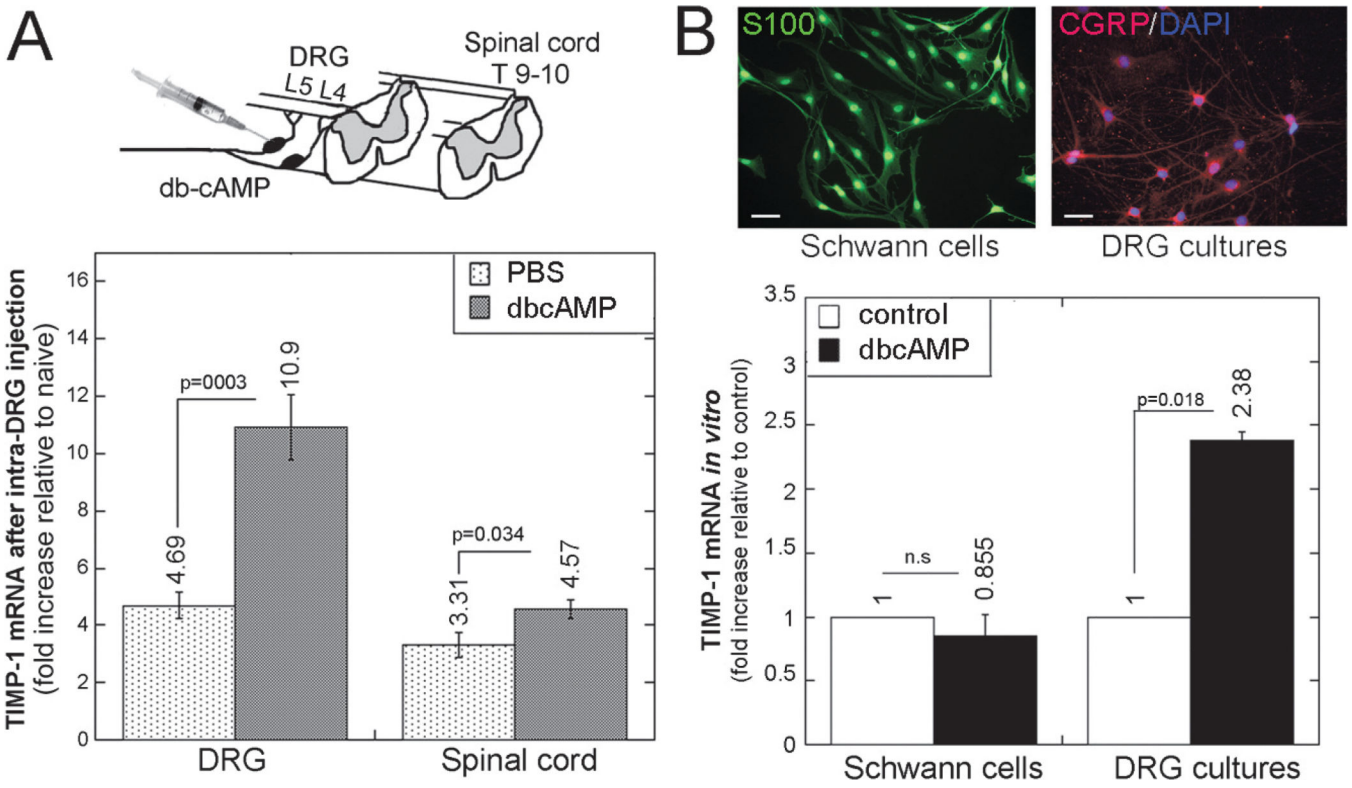

FIGURE 7.

The cAMP analog dbcAMP stimulates TIMP-1 in DRG neurons in vivo and in vitro. **(A)** TaqMan quantitative PCR for TIMP-1 after dbcAMP (50 μg) or PBS injection into the L4 and L5 DRG of naive animals, as shown in experimental schema (top). The graph (bottom) represents the mean ± SEM relative mRNA expression of 4 to 6 animals per group, normalized to GAPDH and calibrated to naive DRG (p values by 1-way ANOVA and Tukey post hoc test). **(B)** S100 immunofluorescence (green; left top) and CGRP immunofluorescence (red; right top) show pure primary Schwann cell cultures and mainly CGRP-positive primary adult DRG cultures, respectively. DAPI, blue. Scale bar = 10 μm. Bottom: TaqMan quantitative PCR for TIMP-1 in Schwann cell or DRG cultures stimulated with dbcAMP (500 μmol/L) or maintained in control media for 24 hours. The graph represents the mean ± SEM relative mRNA of 3 independent experiments and internal duplicate samples, normalized to GAPDH and calibrated to control media (p values by 1-way ANOVA and Tukey post hoc test).

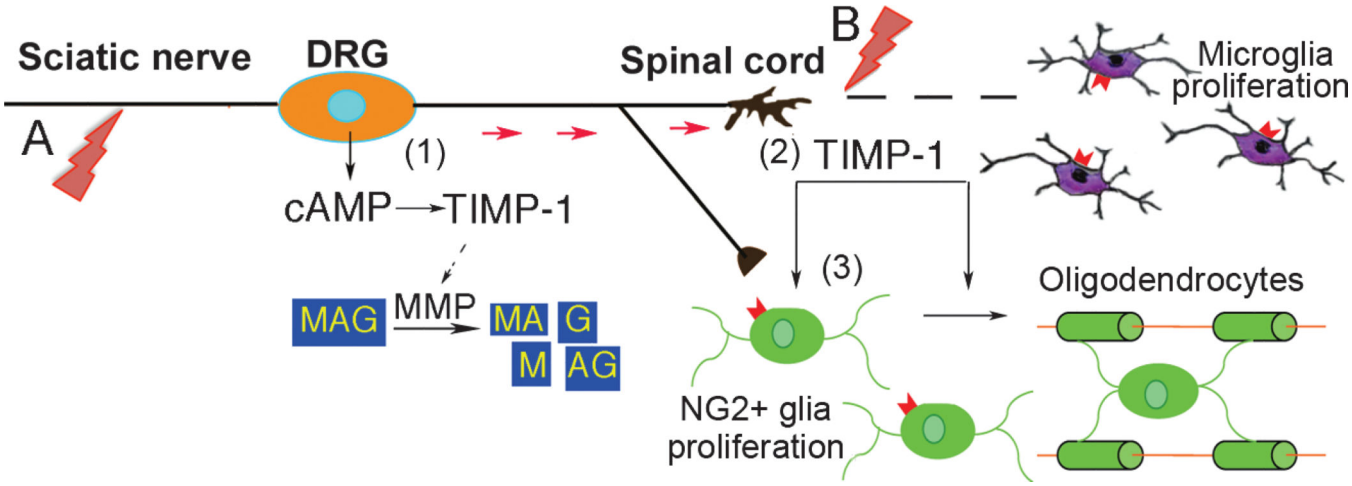

FIGURE 8.

Hypothesis diagram showing how TIMP-1 mediates CNS regeneration after a conditioning PNS lesion. **(A, B)** A DRG neuron shown to be damaged by conditioning sciatic nerve injury **(A)** and subsequent SCI **(B)**. Intraganglionic TIMP-1 production is an element of cAMP-induced regenerative response to PNS injury (1). Tissue inhibitor of metalloproteinase-1 mediates cAMP-stimulated growth of DRG neurons against MAG (2) by blocking proteolytic release of inhibitory MAG peptides (18) and by preventing degradation of permissive substrates (e.g. laminin). Spinal TIMP-1 expression (2) and/or post-Golgi transport of neuronal TIMP-1 (red arrows) stimulates division and subsequent maturation of NG2-positive glia into oligodendrocytes (3) via MMP inhibition (13) and independently of MMPs (31). Together with microglia, dividing NG2-positive glia and cAMP-induced TIMP-1 contribute to PNS injury–induced neurite outgrowth and/or sprouting of central sensory axons.